

Weakening effect of plastic yielding inception in thin hard coating systems

Xiao Huang(黄啸), Shujun Zhou(周述军), and Tianmin Shao(邵天敏)
Citation: Chin. Phys. B, 2021, 30 (**3**): 038104. DOI: 10.1088/1674-1056/abc544
Journal homepage: http://cpb.iphy.ac.cn; http://iopscience.iop.org/cpb

What follows is a list of articles you may be interested in

Effect of AlN coating on hydrogen permeability and surface structure of VT6 alloy by vacuum arc ion plating

Zi-Yi Ding(丁子祎)
Chin. Phys. B, 2019, 28 (**10**): 108101. DOI: 10.1088/1674-1056/ab3a8e

Effect of elasticity mismatch on cell deformation and migration: A phase-field study

Yuanfeng Yin(尹元枫), Hui Xing(邢辉), Duyang Zang(臧渡洋), Kexin Jin(金克新)
Chin. Phys. B, 2018, 27 (**11**): 116201. DOI: 10.1088/1674-1056/27/11/116201

Unusual softening behavior of yield strength in niobium at high pressures

Qiu-Min Jing(敬秋民), Qiang He(何强), Yi Zhang(张毅), Shou-Rui Li(李守瑞), Lei Liu(柳雷), Qi-Yue Hou(侯琪玥), Hua-Yun Geng(耿华运), Yan Bi(毕延), Yu-Ying Yu(俞宇颖), Qiang Wu(吴强)
Chin. Phys. B, 2018, 27 (**10**): 106201. DOI: 10.1088/1674-1056/27/10/106201

Annealing effect of platinum-incorporated nanowires created by focused ion/electron-beam-induced deposition

Fang Jing-Yue, Qin Shi-Qiao, Zhang Xue-Ao, Liu Dong-Qing, Chang Sheng-Li
Chin. Phys. B, 2014, 23 (**8**): 088111. DOI: 10.1088/1674-1056/23/8/088111

Influences of nitrogen flow rate on the structures and properties of Ti and N co-doped diamond-like carbon films deposited by arc ion plating

Zhang Lin, Ma Guo-Jia, Lin Guo-Qiang, Ma He, Han Ke-Chang
Chin. Phys. B, 2014, 23 (**4**): 048102. DOI: 10.1088/1674-1056/23/4/048102

Weakening effect of plastic yielding inception in thin hard coating systems*

Xiao Huang(黄啸)[1], Shujun Zhou(周述军)[1], and Tianmin Shao(邵天敏)[2,†]

[1] School of Mechanical Electronic and Information Engineering, China University of Mining and Technology, Beijing 100083, China
[2] State Key Laboratory of Tribology, Tsinghua University, Beijing 100084, China

(Received 20 August 2020; revised manuscript received 5 October 2020; accepted manuscript online 28 October 2020)

Hard coatings have been widely applied to enhance tribological performance of mechanical components. However, it was predicted that thin hard coatings may have a weakening effect which could reduce the coating/substrate system's resistance to plastic yielding compared with the uncoated substrate material. In this paper, analytical simulation is utilized to investigate the origin of weakening effect. The functions of material mechanical properties and coating thickness on the weakening effect are theoretically investigated. Partial-unloading spherical nanoindentation tests are performed on tungsten coated single crystalline silicon and copper to acquire the stress-strain curves and compared with the uncoated cases. The experimental results are in consistence with the analytical solutions, demonstrating the presence of weakening effect.

Keywords: plastic yielding, weakening effect, spherical nanoindentation, PVD coating

PACS: 81.15.Jj, 62.20.F– **DOI:** 10.1088/1674-1056/abc544

1. Introduction

Hard coatings can effectively improve surface tribological performance, especially in reducing friction and promoting resistance to corrosion and wear.[1,2] Classical wear theory emphasizes surface hardness as the key factor of wear resistance. In the last decades, physical and chemical vapor deposition (PVD and CVD) enabled the fabrication of various hard and even super-hard coatings.[3,4] However, the failure origination of a coating/substrate system in friction and wear is complicated, not only abrasive wear on the top surface but also coating fracture in the subsurface and plastic deformation in the substrate can cause the coating failure.[5–8] Particularly for the PVD and CVD coatings whose thickness ranges from hundreds of nanometers to a few microns, substrate plastic yielding could be the premature failure in a coating/substrate system. The plastic flow of substrate material permits the flexure of coating and induces additional tensile stress in the coating, accelerating the initiation and propagation of cracks within the coating material.[9,10] Therefore, it is significant to promote the plasticity onset threshold of the substrate for enhancing the tribological performance of a coating/substrate system.

The behavior of substrate yielding relates more closely to the coating thickness and substrate properties rather than the coating hardness.[8] Several publications revealed that thin hard coating on soft substrate does not necessarily result in better tribological performance. Conversely, it may cause weakening effect of the resistance to plastic yielding in the substrate due to additional stress. Komvopoulos found that indentation of thin hard coatings on soft substrates may cause higher substrate stresses compared with a non-coated case using the finite element method (FEM).[11] It is worth noting that the hard coating is defined as the coating's elastic modulus and hardness is relatively higher than the substrate. Therefore the weakening effect could extensively exist in any hard coating/substrate systems when the coating thickness is not appropriately designed regardless of the coating deposition techniques. In a following paper, Komvopoulos pointed out such higher stresses have a weakening effect on the threshold to plastic yielding of the coating/substrate system.[12] Sun studied the contact mechanics between a rigid sphere and compliant substrates coated with TiN coating using the FEM.[13] The paper found that the critical load of yielding inception in the coated system is smaller than that of the uncoated substrate, demonstrating that the hard coating weakens the substrate's load carrying capacity. Recently, Goltsberg *et al.*[14,15] studied the plasticity onset in a coated sphere loaded by rigid flat using the FEM. The results showed that the weakening effect is closely related to the elastic modulus mismatch between coating and substrate. Song *et al.*[16] studied the plasticity onset in a coated flat contact with a rigid sphere by the FEM and showed similar result with Ref. [14]. In addition to these theoretical studies, there are also a few experimental investigations of weakening effect. Our previous studies[17,18] qualitatively validated the weakening effect model in Ref. [14] using elastic-plastic index (EPL) and showed experimentally that thin hard coatings can reduce the coated system's re-

*Project supported by the National Natural Science Foundation of China (Grant No. 51705533), the National Science and Technology Major Project of China (Grant No. 2017-VII-0013-0110), the Fundamental Research Funds for the Central Universities, China (Grant No. 2020YQJD17), and the Tribology Science Fund of State Key Laboratory of Tribology (Grant No. SKLTKF18B15).

†Corresponding author. E-mail: shaotm@tsinghua.edu.cn

© 2021 Chinese Physical Society and IOP Publishing Ltd

sistance to plastic yield inception. Afterwards our studies tested the wear properties of TiN and TiAlN coating on different substrates.[19] The results showed that larger modulus and hardness mismatch between coating and substrate could cause the detrimental effect of wear properties. Rebholz *et al.*[20] tested the pin-on-disk wear rate of Ti–Al–B–N coatings on soft stainless steel substrate ($H = 5$ GPa). The experiments indicated that the relatively hard coating with large Young's modulus demonstrated a higher wear rate than the coating with moderate hardness and modulus. As can be seen from the above-mentioned literature, the weakening effect has been theoretically proposed several times by the FEM. However, the FEM has the limitation on the element mesh density, so it could be difficult to simulate the model with the coating thickness in the range of micron and submicron. Meanwhile, the detailed study on the origin and influencing factors of weakening effect is still missing. In this study, by utilizing the image charges method in contact mechanics,[21] the stress distribution in a coated system is evaluated analytically to interpreter the origin and influencing factors of weakening effect. Moreover, the experimental validation of weakening effect is indeterminate. In the preview studies, the authors proved that potential weakening effect existed in coated system using indirect methods.[17,18] In this study, the spherical nanoindentation tests are applied to convert the load-displacement curve into a more meaningful stress-strain curve to identify the yielding point.[22,23] The yielding threshold of coated and uncoated single crystalline silicon are compared directly to validate the credibility of weakening effect. This paper is organized as follows: Section 2 presents the theoretical background of stress simulation and spherical nanoindentation. Section 3 describes the experimental methods, Section 4 give the results of simulation and experiments, and finally the conclusion is provided.

2. Theoretical background

2.1. Plastic yielding in spherical contact

Figures 1(a) and 1(b) schematically show a rigid sphere (radius $= R$) in contact with an uncoated elastoplastic flat and a coated elastoplastic flat, respectively. The classical Hertz theory provides the following relations between contact load P and interference h_e in the case of a homogenous flat elastically deformed by a rigid sphere:

$$P = \frac{4}{3}\frac{ER^{1/2}h_e^{3/2}}{(1-\nu^2)}, \tag{1}$$

where E and ν are the elastic modulus and Poisson' ratio of the flat. The von Mises yielding criterion can be used to determine the elastic-to-plastic transition point in this study as the following expression:

$$\sigma_M = \left\{\frac{1}{2}[(\sigma_1-\sigma_2)^2+(\sigma_2-\sigma_3)^2+(\sigma_1-\sigma_3)^2]\right\}^{1/2}, \tag{2}$$

where σ_M is the von Mises stress, σ_1, σ_2, and σ_3 are the principal stresses. When σ_M exceeds the yielding strength Y of the flat material, the plastic yielding occurs. Combined the Hertz theory and von Mises criterion, the critical load that initiates the plastic yielding in a homogenous flat can be expressed as[15]

$$P_c = \frac{\pi^3}{6}C_\nu^3 Y\left(R(1-\nu^2)\frac{Y}{E}\right)^2, \tag{3}$$

where C_ν is the function of Poisson's ratio in the form of $C_\nu = 1.234 + 1.256\nu$.

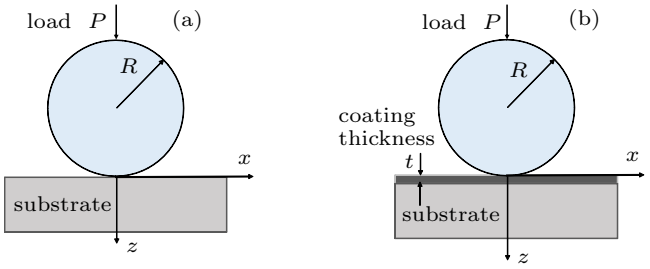


Fig. 1. Schematic of spherical contact. (a) uncoated surface (b) coated surface.

However, when the homogenous flat is coated, the Hertz theory is no more valid to evaluate the stress distribution. In this study, the stress distribution and plastic yielding inception in the coated flat is solved by commercial FilmDoctor software. The software is based on the image charges method, which is well-known in electrodynamics. The image charges method is completely analytical which can be expressed in elementary functions and closed form.[21,24] In contact mechanics, the method treats all the surfaces and interfaces as boundaries where special stress and strain conditions should be satisfied. In this study, the interface between coating and substrate is assumed to be well-bonded, therefore, the displacement, the stress normal to the interface and the shear stress are identical at both sides of the interface. The stress parallel to the interface and the strains are different at two sides of the interface. Based on the above boundary conditions, the principal stresses along the depth are evaluated and simultaneously used to calculate the von Mises stress to determine the yielding point. The load-displacement relation solved by FilmDoctor was compared with the Hertz theory to verify the accuracy of the software. The difference between two methods is less than 0.5% which is more accurate than the FEM with the error of 2.5%.

2.2. Nanoindentation stress-strain curve

Figure 2 schematically shows the geometry of a spherical nanoindentation test. The total interference h_t consists of elastic portion h_e and plastic portion h_p. The widely used Oliver and Pharr method utilizes the unloading slope to determine

the h_e by differentiating Eq. (1) with respect to h and yields the following expression:

$$\frac{dP}{dh} = 2ER^{1/2}h_e^{1/2}. \tag{4}$$

Substitute Eq. (4) to Eq. (1) to result the following expression:

$$P = \frac{2}{3}\frac{dP}{dh}h_e, \tag{5}$$

where dP/dh is the stiffness S of the unloading part of the indentation load-displacement curve, which can be determined from the unloading slope. Therefore, the h_e can be evaluated by the following expression:

$$h_e = \frac{3}{2}\frac{P}{S}. \tag{6}$$

Once h_e is determined, the contact depth h_c can be calculated. The contact depth h_c is defined as the distance from the contact point to the maximum interference. Sneddon[25] showed that the elastic interferences above and below the contact point are equal to each other. Therefore, h_c could be given in the following expression:[26]

$$h_c \approx h_t - \frac{h_e}{2}. \tag{7}$$

Afterwards, the contact radius a can be given by

$$a = \sqrt{2Rh_c - h_c^2} \approx \sqrt{2Rh_c}. \tag{8}$$

Note that h_e equals h_t within the elastic limit, so the indentation radius a can be simplified to $a^2 = h_e \cdot R$ when the deformation is purely elastic. Combining Eqs. (1) and (8) yields

$$\frac{P}{\pi a^2} = \frac{4}{3\pi}E\left(\frac{a}{R}\right). \tag{9}$$

Assuming indentation stress $\sigma = \frac{P}{\pi a^2}$ and indentation strain $\varepsilon = a/R$, the linear relationship between σ and ε is expected within the elastic limit. Therefore, the plastic yielding inception can be identified when the stress-strain curve deviates from linear correlation.

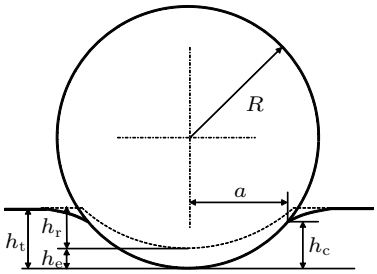


Fig. 2. Schematic of spherical nanoindentation.

The above theory is based on the spherical indentation test on a homogenous flat. When the flat is covered with coating, the linear relationship between σ and ε is still valid, but the ratio between σ and ε is determined by the effective modulus which is the function of the moduli of both coating and substrate and coating thickness.

3. Experimental details

3.1. Specimen preparation

The (100)-oriented single-crystalline silicon wafer and polished copper were used as substrates for coating deposition. Tungsten (W) coatings were deposited on silicon and copper substrates by an ion beam assisted deposition (IBAD) system.[27] with the thickness of 700 nm and 600 nm respectively. In the IBAD system, the assisted ion beam could impact the coating atoms onto the substrate to improve the binding force between coating and substrate. For the deposition process, the vacuum chamber was first exhausted to a base vacuum pressure of 3.5×10^{-4} Pa to remove impurity gases. Following this, working gas Ar was introduced into the chamber and pressurized to 1.0×10^{-2} Pa to start the ion arc. The substrates were bombarded by the assist ion source for 10 min for decontamination prior to the coating process. During the deposition process, the working current of the ion sources was 80 mA with energy of 2500 eV. In order to obtain uncoated specimens for comparison, several silicon and copper samples were masked with tin foil and placed adjacent to the samples to be coated. This was carried out to avoid possible heat induced differences between the coated and uncoated samples.

3.2. Properties of measurement

The nanohardness and elastic modulus of the tungsten coating, the silicon substrate and the copper substrate were measured by the nanoindentation system (CSM Instrument Nanoindentation Tester NHT2) using pyramidal Berkovich tip with a force of 2 mN. For the nanohardness and elastic modulus tests, 20 repetitions were carried out in a 4×5 matrix and 20 μm apart. Poisson's ratio of the silicon, copper and tungsten coating is assumed to be 0.3 in the modulus measurements. The surface roughness is measured using an interferometer (ZYGO NewView 8200).

3.3. Spherical nanoindentation

Spherical indentation tests were utilized to derive stress-strain relations from common load-displacement curves as discussed in Section 2.3. The tests were also carried out on the CSM NHT2 nanoindentation system using a spherical diamond tip with the radius of 20 μm. The partial unloading mode was applied[28] in the test, during which the maximum load was not applied in a single loading segment. Instead, repeated loading-unloading loops were performed with gradually increasing load to accomplish the entire loading process as shown in Figs. 3(a) and 3(b). The unloading stiffness S can be derived from each loading-unloading loop and is further used to determine the stress and strain at each load value. The maximum load on the coated/uncoated silicon is 450 mN with 100

loading-unloading cycles and 25 mN on the coated/uncoated copper with 15 cycles since the copper has a much lower elastic limit than the silicon. Five indentation repetitions were carried out to obtain the average results. After indentation tests, a scanning electron microscope (SEM, TESCAN LYRA3) and a focused ion beam (FIB, TESCAN LYRA3) were used to observe the top surface and cross-section of the indention dots to confirm if there is any fracture or delamination in the coating or substrate or at the coating/substrate interface.

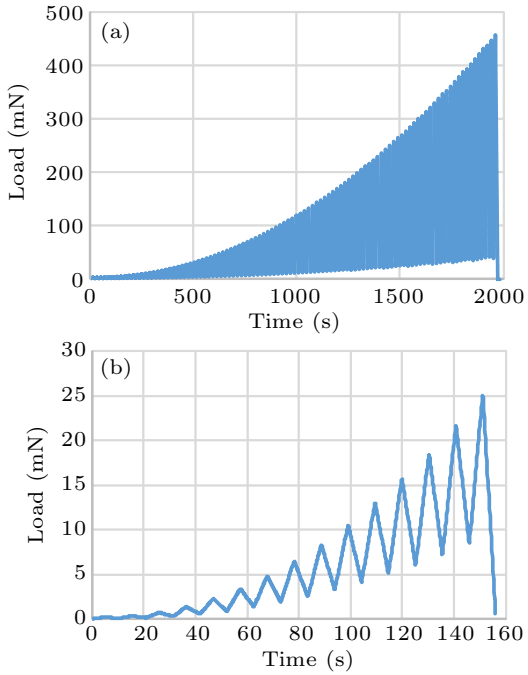


Fig. 3. Load evolution in partial unloading nanoindentation test: (a) maximum 450 mN on silicon, (b) maximum 25 mN on copper.

4. Results and discussion

4.1. Origin of weakening effect

The von Mises stress criterion was adopted in the plastic yielding judgement in both uncoated and coated substrates. FilmDoctor was used to calculate the maximum von Mises stress inside the substrate material. In order to verify if FilmDoctor's calculation is accurate, the simulation results is compared with classic Hertz solution and published finite element method (FEM) simulation results,[15] which also focused on the weakening effect. The comparison comes out that FilmDoctor's analytical simulation has good fits with the Hertz solution and the published FEM results. Thus the simulation results by FilmDoctor should be reliable. Table 1 gives the typical calculation instance of material properties. In the calculation, the coating thickness is 2 μm and the substrate thickness is 100 μm to eliminate possible influence from the bottom support. When the von Mises stress exceeds the substrate's yielding strength, the plastic deformation occurs and the corresponding load is marked as the critical load P_c.

Table 1. Input material properties for calculation.

	Substrate	Coating	Contact ball
Young's modulus E (GPa)	100	200	1140
Yielding strength Y (MPa)	200	–	–
Poisson's ratio ν	0.3	0.3	0.07
Thickness or Radius (μm)	Semi-infinite	2	1000

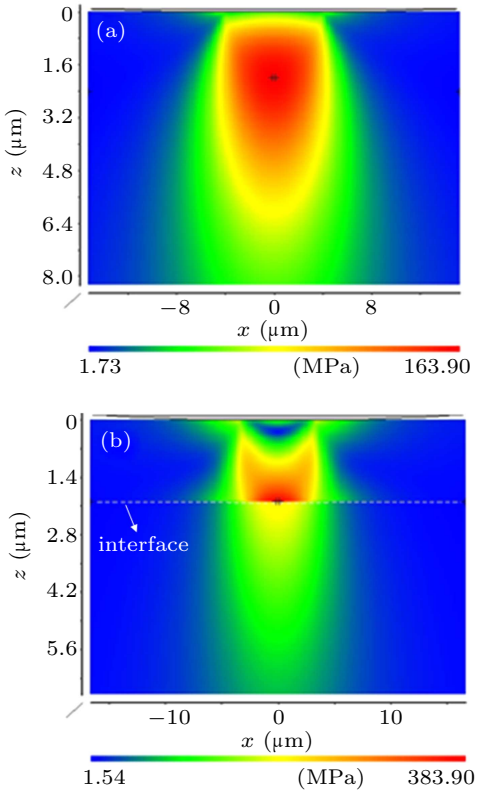


Fig. 4. The von Mises stress distribution for (a) the uncoated substrate and (b) the coated system.

The calculated P_c of the uncoated and coated substrate is 17 and 9.5 mN respectively, indicating the presence of weakening effect. Figures 4(a) and 4(b) show the von Mises stress distribution in uncoated and coated cases at the same load $P = 9.5$ mN. Overall, the von Mises stress is continuous in the uncoated substrate. Since the applied load (9.5 mN) is below the yielding critical load (16 mN) of the uncoated substrate, the maximum stress (163.9 MPa) is still within the elastic limit (200 MPa). The maximum stress is located in the subsurface, which is in accordance with the Hertz theory. By contrast, the von Mises stress is discontinuous at the coating/substrate interface in the coated system. The maximum stress (383.9 MPa) is located at the interface inside the coating. Since the PVD coating is much harder than the substrate material, such mild stress cannot initiate plastic yielding in the coating material. However, the von Mises stress in the substrate just reaches the yielding strength (200 MPa) along the interface inside the substrate. Thus the hard coating does not efficiently protect the substrate from plastic yielding and even introduces a weakening effect of loading bearing capacity.

Figure 5 shows the principle stress along the depth at the position of symmetry axis. Notice that along the symmetry

axis the shear stresses are all zero ($\tau_{xy} = \tau_{xz} = \tau_{yz} = 0$), so the principle stress equals the corresponding normal stress, i.e., $\sigma_z = \sigma_1$ and $\sigma_x = \sigma_y = \sigma_2 = \sigma_3$. Under the above conditions, the calculation of von Mises stress can be reduced to the following equation $\sigma_{von} = |\sigma_1 - \sigma_2| = |\sigma_z - \sigma_x|$. In the uncoated substrate, σ_x, σ_y and σ_z are continuous and negative, indicating the substrate are in compressive stress state. In contrast, in the coated substrate system, σ_x and σ_y are discontinuous at the coating/substrate interface while the σ_z remains continuous. In the substrate close to the interface, the σ_x increases from -50 MPa without coating to -30 MPa with coating, while the σ_z decreases from -210 MPa to -230 MPa. The opposite trend leads to larger gap between σ_x and σ_z in the coating/substrate system compared to the uncoated substrate. As discussed above, the calculation of von Mises stress can be simplified to the difference between σ_x and σ_z, thus the von Mises magnifies in the coating/substrate system.

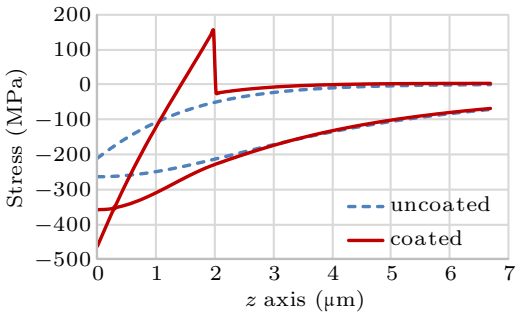


Fig. 5. Principle stress distribution along the z axis

To further explore the reason of stress growth in the coated system, Figs. 6 and 7 show the normal displacement and strain along the z axis. The normal displacement along the z axis in coated system is continuous at the coating/substrate interface. This is due to the well-bonding between coating and substrate, so the displacement is compatibility at the interface. There is a significant inflection of normal displacement at the interface as shown in Fig. 6, so the differential coefficient of displacement, namely the normal strain should be discontinuous at the interface. The result in Fig. 7 coincides with the deduction, the normal strain is discontinuous at the interface. According to the generalized Hooke law, the relation between stress and strain is as follows:

$$\varepsilon_z = \frac{1}{E}[\sigma_z - \nu(\sigma_x + \sigma_y)]. \tag{10}$$

Equation (10) can be further converted to the following expression:

$$\sigma_x = \sigma_y = \frac{1}{2\nu}(\sigma_z - E\varepsilon_z). \tag{11}$$

According to Eq. (11), with the decrease of ε_z, the tendency of σ_x is rising. Indeed, Figs. 5 and 7 demonstrate the ε_z decreases and σ_x increases in the coated system. Since the principal stress σ_x is positive, the increasing σ_x means that the principal stress becomes more tensile. Meanwhile, when a hard coating/substrate system is contacted by an indenter, the contact area is smaller than the uncoated substrate and this will cause the principal stress σ_z more compressive. This means that the algebraic value of σ_z decreases. The opposite change tendency of σ_x and σ_z causes the rise of von Mises stress as shown in Fig. 5. It is worth noting that in Eq. (11) σ_z also has a function on the value of σ_x. In the coated system, the decreasing σ_x could counteract the decreasing ε_z and further influences the weakening effect. Thus the influencing factors of weakening effect are complex and will be discussed in detail in Subsection 4.2. Note that weakening effect is caused by the additional stress at the coating/substrate interface under contact force. Different coating technology would not have significant effect on the weakening effect. Whenever the coating's modulus is higher than the substrate and the coating thickness is inappropriate designed, the weakening effect could exist.

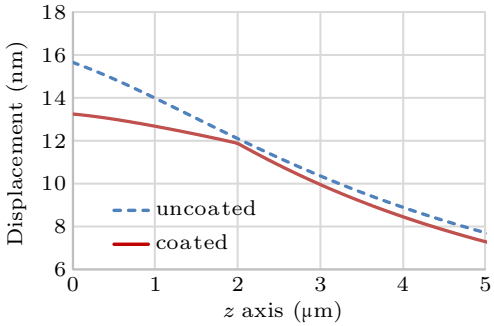


Fig. 6. Normal displacement along the z axis.

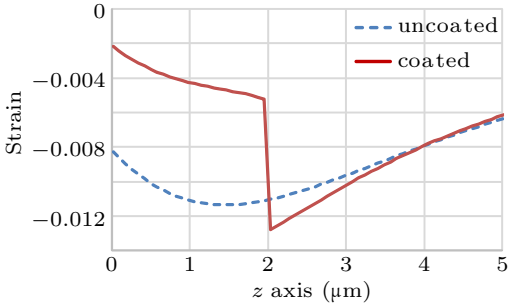


Fig. 7. Normal strain ε_z along the z axis.

4.2. Influencing factors of weakening effect

The calculation of P_c requires the dimensional input of specific material properties, such as elastic modulus, yielding strength and coating thickness. In order to acquire the universal dimensionless solution of weakening effect, a wide range of material properties are taken into consideration. The radius R of the spherical diamond tip is set to be 100 μm. The coating thickness t varies from 0.1 to 10 μm, yielding the dimensionless t/R ratio in the range of $0.001 \leq t/R \leq 0.1$. The elastic moduli of the coating and substrate vary in the range $300 \leq E_{co} \leq 800$ GPa and $100 \leq E_{su} \leq 600$ GPa. The yielding

strength of the substrate varies in the range $0.3 \leq Y_{su} \leq 1$ GPa. The coating material is assumed to be purely elastic in this study to simplify the calculation. Poisson's ratio of both coating and substrate is set to be 0.3, which has neglected the effect on the calculation results.

As shown in Table 2, eight typical substrate and coating combinations were selected to demonstrate the influencing factors of weakening effect. The calculation were carried out by FilmDoctor and the results are shown in Fig. 8. In Figs. 8(a) and 8(b), the curves labeled with 1–4 and 5–8 are corresponding to the parameters 1–4 and 5–8 in Table 2, respectively. The x axis in Fig. 8 is the dimensionless coating thickness (t/R), namely the ratio between coating thickness (t) and radius (R) of the counterpart. The y axis (P_c) is the dimensionless critical load of plastic yielding, which is the ratio between the critical load of coated system (P_{c_sys}) and uncoated substrate (P_{c_sub}), namely $P_c = P_{c_sys}/P_{c_sub}$. When P_c is below 1, the coated system has a less resistance to plastic yielding compared to the uncoated substrate, so the weakening effect exists. In reverse, whenP_c is above 1, the weakening effect vanishes and turns to a strengthening effect. Figure 8 shows that with the increasing coating thickness (t/R), the critical load P_c decreases at the early stage and then increases. The minimum P_c signifies a poor design of coating thickness and the weakening effect is most severe at such a coating thickness. Therefore, the minimum P_c is marked as P_{c_mw} and the corresponding dimensionless coating thickness is marked as $(t/R)_{mw}$. With the increasing of coating thickness, P_c goes beyond 1, so the weakening effect vanishes and transfers to strengthening effect. Thus the coating thickness at the transferring point is marked as $(t/R)_T$.

Table 2. Mechanical properties of coating/substrate combinations.

	1	2	3	4	5	6	7	8
E_{co} (GPa)	400	400	400	400	800	800	800	800
E_{sub} (GPa)	200	200	200	200	200	200	200	200
Y_{sub} (GPa)	0.4	0.6	0.8	1.0	0.4	0.6	0.8	1.0
P_{c_sub} (mN)	0.41	1.38	3.38	6.40	0.41	1.38	3.38	6.40

Figure 8(a) shows that P_{c_mw} in combinations 1–4 are identical and the value is about 0.64, which means that the coated system's threshold to plastic yielding is 36% lower than the uncoated substrate. Similarly, the P_{c_mw} values in Fig. 8(b) are also identical to each other, i.e., about 0.5. Therefore, the P_{c_mw} is determined by the elastic modulus mismatch between coating and substrate, E_{co}/E_{sub}. The larger the modulus mismatch is, the more severe the weakening effect may occur. By simulating a series of E_{co}/E_{sub} combinations, it is found that the relation between P_{c_mw} and E_{co}/E_{sub} can be summarized in the following equation:

$$P_{c_mw} = 0.2884 + \frac{0.4614}{E_{co}/E_{sub} - 0.356}. \tag{12}$$

In a similar way, $(t/R)_{mw}$ can be expressed as follows:

$$(t/R)_{mw} = \frac{1}{(E_{sub}/Y_{sub})(E_{co}/E_{sub})^{0.2528}}. \tag{13}$$

Equation (13) shows that $(t/R)_{mw}$ decreases as E_{co}/E_{sub} increases. The $(t/R)_{mw}$ represents the dimensionless coating thickness corresponding to the most-weakening effect. Therefore the worst coating thickness becomes smaller when E_{co}/E_{sub} increases.

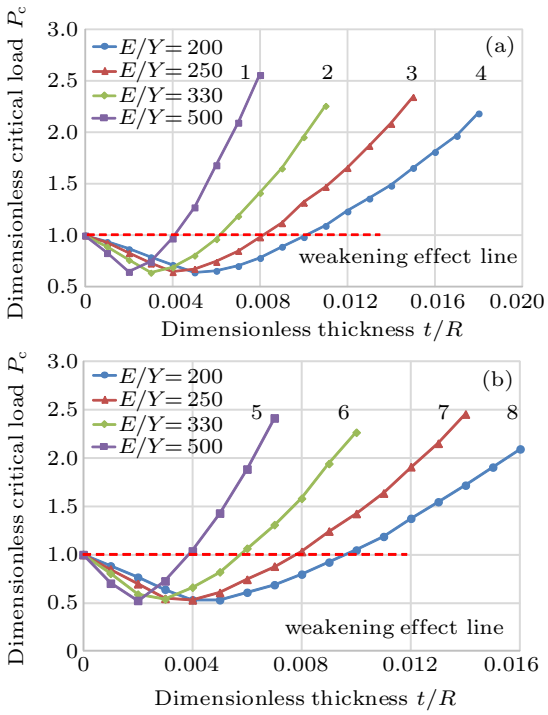


Fig. 8. Relation between P_c and (t/R) in different coating/substrate systems: (a) $E_{co}/E_{sub} = 2$, (b) $E_{co}/E_{sub} = 4$.

Similarly, the transition thickness $(t/R)_T$ from weakening effect to strengthening effect can be expressed in the following equation:

$$(t/R)_T = \begin{cases} [0.8374 + (E_{co}/E_{sub} - 1)^{0.1954}](Y_{sub}/E_{sub}), & E_{co}/E_{sub} < 2.5, \\ (0.02026 - 0.0005408 \cdot E_{co}/E_{sub})(Y_{sub}/E_{sub}), & E_{co}/E_{sub} \geq 2.5. \end{cases} \tag{14}$$

Equation (14) shows that $(t/R)_T$ is determined by both E_{co}/E_{sub} and Y_{sub}/E_{sub}, yet Y_{sub}/E_{sub} has a much more significant effect than E_{co}/E_{sub}.

Using Eqs. (12)–(14), the critical coating thickness $(t/R)_T$, the most weakening effect P_{c_mw} and the corresponding coating thickness $(t/R)_{mw}$ in any given coating/substrate system can be easily calculated to guide the design of a coating system.

4.3. Indentation stress-strain curves

Table 3 shows the mechanical properties and surface roughness of the samples. The W coating is harder and more rigid than silicon and copper substrates. Using FilmDoctor, it is confirmed that 700 nm W coating on silicon and 600 nm W coating on copper both have weakening effect. The silicon, copper and W coating are nanometer scale smooth, which is suitable for performing nanoindentation tests.

Table 3. Properties of the samples.

	Silicon substrate	Copper substrate	W coating
Nanohardness (GPa)	12.6	1.4	19.9
Young's modulus (MPa)	172.7	113.1	262.2
Roughness (nm)	2	17	11

Using partial unloading nanoindentation test as described in Subsection 3.3, stress-strain test results are illustrated in Figs. 9(a)–9(d). The tests on uncoated silicon wafer have a good repeatability since the wafer surface is nanometer level smooth. The curves in Fig. 9(a) does not start from the coordinate origin since a certain stress and strain have been generated at the first indentation point. The red dotted line in Fig. 9(a) is obtained by extending the linear relation of the stress-strain curve from the coordinate origin as a reference line. The spherical indentation induced plastic deformation in monocrystalline silicon is not as obvious as that in metal tensile test since the stress field produced by spherical indentation is unique.[29] The maximum von Mises stress beneath spherical indenter is located in the subsurface instead of the top surface. Thus the plastic zone is fully surrounded by the elastic zone, which has a limited influence on the stress-strain curve. With the increasing loading force, the plastic zone gradually expands and stress-strain relationship gradually deviates from the linear relationship. It is worth noting that the plastic deformation in silicon is caused by phase transformation rather than dislocation slip. The crystalline silicon can transfer to amorphous silicon under certain contact stress. Since the amorphous silicon is less rigid than the crystalline silicon and thus exhibits a similar plastic yielding phenomenon in the stress-strain curve. In the uncoated wafer, when the strain value exceeds 0.1 (the corresponding load is about 120 mN), the stress-strain curve shows certain plasticity. In Fig. 9(b), the repeatability of tests on coated silicon is slightly lower, which may be caused by the higher surface roughness of the coated sample. There is a linear relationship between stress and strain at the beginning of the curves. When the strain value exceeds 0.08 (the corresponding loading force is about 100 mN), the curves deviate from linear relationship.

Figures 9(c) and 9(d) show the stress-strain curves on coated and uncoated copper. Since copper has a relatively larger roughness and less homogeneity than silicon wafer, the fluctuation in the stress-strain curves on copper is more obvious than silicon. Nevertheless, Figs. 9(c) and 9(d) show that the uncoated and coated copper deviate from linear relationship when the strain exceeds 0.025 (the corresponding loading force is about 3.0 mN) and 0.02 (the corresponding loading force is about 2.5 mN), respectively. Therefore the weakening effect is also valid in the coated copper.

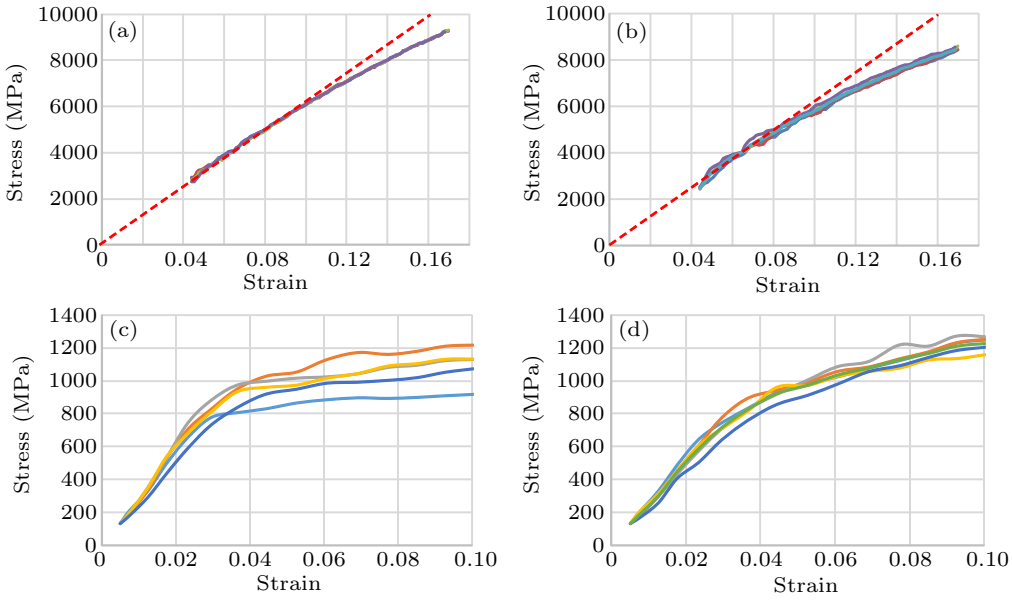


Fig. 9. Nanoindentation stress-strain curves: (a) uncoated silicon, (b) coated silicon, (c) uncoated copper, (d) coated copper.

For further comparison, Fig. 10 illustrates the average results of the above stress-strain tests. In Fig. 10(a), when the strain value is less than 0.08, the two curves are basically coincident. When the strain exceeds 0.08, the coated silicon undergoes plastic deformation first, and the uncoated silicon keeps elastic deformation until strain exceeds 0.10. The de-

gree of plastic deformation in the coated silicon is more severe than the uncoated silicon. Therefore the tungsten coated silicon has a weakened threshold of plastic deformation than the uncoated silicon, indicating the existence of weakening effect. In Fig. 10(b), the two curves deviate gradually when the strain exceeds 0.01 and the dashed line is above the solid line until strain exceeds 0.05, indicating the coated copper already emerged mild plastic yielding at strain point of 0.01. Meanwhile, the solid line deviates from linear relation when strain exceeds 0.02, indicating that the plastic deformation becomes obvious in the coated copper at the strain point of 0.02. In the uncoated copper, the corresponding point is around strain point of 0.025. The above two phenomena once again indicate that the weakening effect is valid in coated copper. Note that the solid line exceeds the dashed line when the strain is over 0.05. This could be caused by the work hardening under severe plastic deformation which is not the research focus in this study.

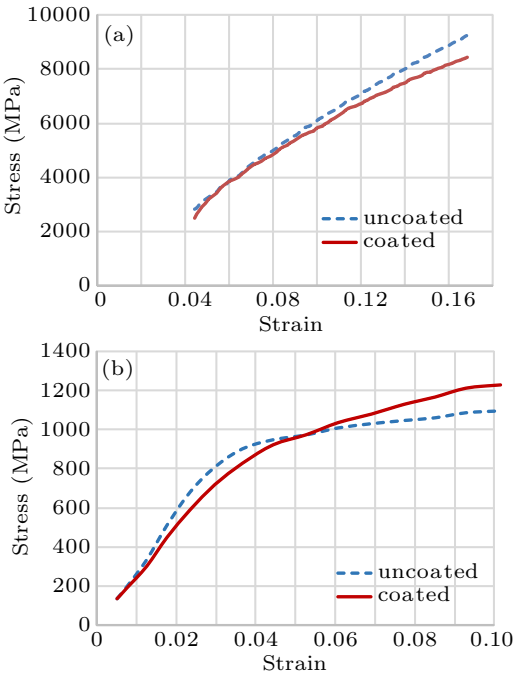


Fig. 10. Average stress-strain curves: (a) coated and uncoated silicon, (b) coated and uncoated copper.

In Fig. 11, SEM and FIB were applied to check the top surface and cross section of the indentation dots to verify if there is any fracture in the coating or debonding at the coating/substrate interface. In the SEM images, the coating and substrate seem to be intact and free from obvious fractures. The coating and substrate is also well bonded without obvious delamination. Thus the fracture and delamination may have negligible effect on the indentation tests. The weakening effect in the stress-strain curves should be caused by the plastic yielding inception in the substrate.

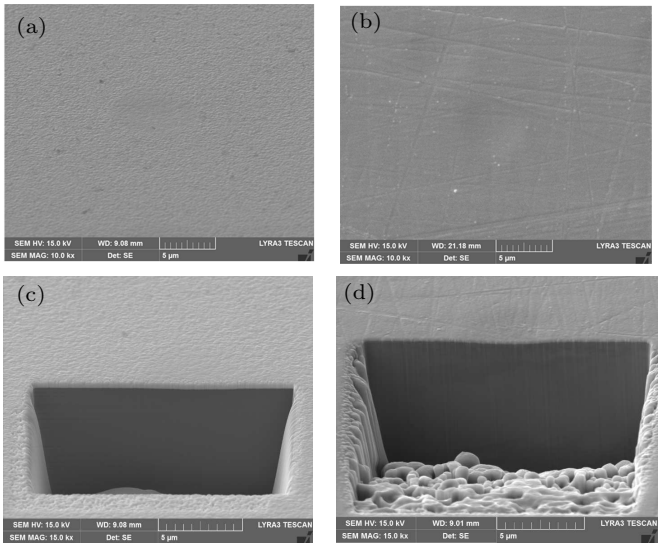


Fig. 11. Top surface and cross-section SEM of nanoindentation dots: (a) top surface of W coated silicon, (b) top surface of W coated copper, (c) cross section of W coated silicon, (d) cross section of W coated copper.

5. Conclusions

The stress-strain curves of monocrystalline silicon wafers and polished copper have been obtained using partial-unloading spherical nanoindentation tests. The tungsten coated silicon and copper demonstrate a weakening effect of plastic yielding threshold compared with the uncoated samples. This may be the first direct validation of the weakening effect in hard coating systems. The origin of weakening effect is analyzed by stress simulation and the results indicate that the modulus mismatch between coating and substrate could induce extra stress in coating systems and cause the early plastic yielding in coating systems. The dimensionless formula of influencing factors on weakening effect is induced by stress simulation and numerical fitting, which can theoretically guide the optimization design of hard coating systems.

References

[1] Veprek S and Veprek-Heijman M J G 2008 *Surf. Coat. Technol.* **202** 5063
[2] Zhang G L, Wang J L, Liu Y F, Liu C Z and Yang S Z 2004 *Chin. Phys. B* **13** 1309
[3] Sarakinos K, Alami J and Konstantinidis S 2010 *Surf. Coat. Technol.* **204** 1661
[4] Liu S W, Wang H P, Xu Q, Ma T B, Yu G, Zhang C, Geng D, Yu Z, Zhang S, Wang W, Hu Y Z, Wang H and Luo J 2017 *Nat. Commun.* **8** 14029
[5] Borrero-López O, Hoffman M, Bendavid A and Martin P J 2008 *Acta Mater.* **56** 1633
[6] Jungk J M, Michael J R and Prasad S V 2008 *Acta Mater.* **56** 1956
[7] Sun Y, Bloyce A and Bell T 1995 *Thin Solid Films* **271** 122
[8] Michler J and Blank E 2001 *Thin Solid Films* **381** 119
[9] Kot M, Rakowski W, Lackner J M and Major 2013 *Mater. Design* **43** 99
[10] Xie Z H, Hoffman M, Moon R J and Munroe P R 2006 *J. Mater. Res.* **21** 437
[11] Komvopoulos K 1988 *J. Tribol.* **110** 477
[12] Komvopoulos K 1989 *J. Tribol.* **111** 430
[13] Sun Y, Bloyce A and Bell T 1995 *Thin Solid Films* **271** 122

[14] Goltsberg R and Etsion I 2013 *Wear* **308** 10
[15] Goltsberg R, Etsion I and Davidi G 2011 *Wear* **271** 2968
[16] Song W, Li L, Ovcharenko A, Jia D, Etsion I and Talke F E 2012 *Tribol. Int.* **53** 61
[17] Huang X, Etsion I and Shao T 2015 *Wear* **338–339** 325
[18] Huang X, Kasem H, Shang H F, Shao T M and Etsion I 2012 *Wear* **296** 590
[19] Huang X, Etsion I and Shao T 2015 *Wear* **338–339** 54
[20] Rebholz C, Ziegele H, Leyland A and Matthews A 1998 *J. Vacuum Sci. Technol. A* **16** 2851
[21] Schwarzer N 2000 *Surf. Coat. Technol.* **133–134** 397
[22] Kalidindi S R and Pathak S 2008 *Acta Mater.* **56** 3523
[23] Pathak S and Kalidindi S R 2015 *Mater. Sci. Engin.: R* **91** 1
[24] Schwarzer N 2000 *J. Tribol.* **122** 672
[25] Sneddon I N 1965 *Int. J. Engin. Sci.* **3** 47
[26] Oliver W C and Pharr G M 2004 *J. Mater. Res.* **19** 3
[27] Wei S, Shao T and Ding P 2010 *Diamond Relat. Mater.* **19** 648
[28] Basu S, Moseson A and Barsoum M W 2006 *J. Mater. Res.* **21** 2628
[29] Muhammad I, Fayyaz H, Muhammad R and Ahmada S A 2012 *Chin. Phys. B* **21** 116201